A Laboratory Study of NMR Relaxation Times and Pore Coupling in Heterogeneous Media

Running Title:
NMR Relaxation Times and Pore Coupling

Elliot Grunewald (elliotg@stanford.edu)
Department of Geophysics, Stanford University

Rosemary Knight (rknight@stanford.edu)
Department of Geophysics, Stanford University

Revised for publication in
Geophysics
April 23, 2009

ABSTRACT

This laboratory study investigates the link between nuclear magnetic resonance (NMR) relaxation times and pore geometry in heterogeneous media. For materials with well-connected pores, this relationship is poorly understood due to a phenomenon known as pore coupling which arises when diffusing protons sample multiple pores before relaxing. Our experiments explore how surface geochemistry influences pore coupling and how this process affects the observed relaxation-time distribution. We measure the NMR response of microporous silica gel packs treated with varying amounts of surface-coating iron and find that samples with less iron exhibit stronger pore coupling than those with abundant iron. When pore coupling is strong, the relaxation-time distribution grossly misrepresents the underlying bimodal pore-size distribution of micropores and macropores. Specifically, as coupling increases, the bimodal relaxation time distribution becomes merged and the relative amplitude of the peaks fails to reflect the true macropore and micropore volume. We attribute a reduction in pore coupling, observed with increasing iron content, to a decrease in the distance protons are able to diffuse before relaxing. Basic parameters describing the shape of the relaxation-time distributions for this range of samples are well-predicted by a 1D analytical model. Our experimental results conclusively demonstrate that surface geochemistry is an important factor determining the degree to which pore coupling occurs and illustrate how this phenomenon can affect the interpretation of NMR relaxation measurements in heterogeneous porous media.

INTRODUCTION

Nuclear magnetic resonance (NMR) relaxation measurements provide an unparalleled view into the pore space of geologic materials. The proton NMR method probes the time required for hydrogen nuclei in the pore water to relax to equilibrium through diffusion and interaction with the pore-scale physiochemical environment. NMR relaxation-time measurements have been utilized for decades in geophysical well-logging to estimate hydrocarbon reservoir properties such as porosity, pore-size distribution, and permeability [Seevers, 1966; Kenyon et al., 1988; Straley et al., 1995]. More recent research has extended NMR geophysical techniques to near-surface environmental applications and has led to the development of a surface-based NMR method, magnetic resonance sounding (MRS), used to measure the NMR response of groundwater aquifers [Legchenko and Valla, 2002; Hertrich, 2008; Walsh, 2008]. This study seeks to improve the interpretation of near-surface NMR measurements by exploring the link between NMR relaxation-times and pore-scale properties in heterogeneous porous media.

The analysis of NMR relaxation measurements in geologic materials requires an accurate model of the physical processes governing relaxation. Conventional interpretation of these data assumes a model of isolated pores in which each diffusing proton samples only one pore. Thus, it is assumed that each pore contributes independently to the NMR signal, with a characteristic relaxation time. In many near-surface materials, however, pores are sufficiently connected that diffusing protons can readily sample multiple pores during the NMR measurement. For materials in which pores are strongly coupled by diffusion, the resulting relaxation-time distribution reflects a complex averaging of the pore network that can be difficult to interpret.

Understanding the conditions in which pore coupling occurs and how this process can influence the NMR relaxation measurement is clearly fundamental to the successful utilization of NMR data in geophysical applications. A number of studies have explored this issue theoretically using models of idealized pore networks to determine how factors such as pore geometry [Cohen and Mendelson, 1982; McCall et al., 1991; Zielinski et al., 2002] and surface geochemistry [Ramakrishnan et al., 1999, 2001] might control the extent of pore coupling. Despite the clear need to account for pore coupling effects, relatively few laboratory studies have explored this phenomenon. Toumelin et al. [2002] showed that interpore diffusion can strongly influence NMR measurements in carbonates and noted that the degree of coupling generally increases with temperature as the pore fluid diffusivity increases. More recently, Anand and Hirasaki [2007] investigated geometric controls on pore coupling in microporous grain packs, and found that coupling between micropores and larger intergranular pores becomes more significant as the grain diameter decreases. However, no laboratory study to date has explored the geochemical controls on pore coupling that were suggested by Ramakrishan [1999].

The aims of this study are two fold: first, to improve our understanding of the geochemical controls on pore coupling, and secondly, to determine how the coupling process affects the interpretation of NMR relaxation measurements. We first seek to establish that surface geochemistry can, in fact, control the strength of pore coupling. In our laboratory approach, we study a well-characterized porous media, silica gel, and measure the NMR response of samples with varied geochemistry. Utilizing a demonstrated link between surface-iron concentration and pore coupling strength, we then aim to identify the specific effects of pore coupling on the relaxation time distribution. Finally, we are able to compare our experimental results with theoretical predictions from Ramakrishnan et al. [1999]. This study of NMR

relaxation measurement in a controlled system contributes to our ultimate goal of improving the interpretation of NMR measurements in heterogeneous near-surface sediments.

BACKGROUND

In the NMR relaxation experiment, a static magnetic field is applied to a water-saturated sample causing an equilibrium alignment of the magnetic moments associated with protons in the pore water. The system is then perturbed by a secondary radio-frequency pulse which excites the protons to a higher energy state, and the magnetization (M) is monitored over time as the system relaxes to equilibrium. There are two time constants describing NMR relaxation: T_1 and T_2. The longitudinal relaxation rate T_1^{-1}, is the rate at which the protons return to their equilibrium state. In the commonly assumed case of fast diffusion (Senturia and Robinson [1970]), the net observed relaxation rate T_1^{-1} for a single pore is given by

$$T_1^{-1} = T_{1B}^{-1} + \rho_1 \left(S / V \right) \tag{1}$$

where T_{1B}^{-1} is the relaxation rate of the bulk water, S/V is the surface area to volume ratio of the pore, and ρ_1 is the longitudinal surface relaxivity [Brownstein and Tarr, 1979]. Surface relaxivity is a geochemical property describing the capacity of the grain surface to enhance relaxation and generally increases with the concentration of paramagnetic impurities on a surface (e.g. Mn^{2+} or Fe^{3+}) [Foley et al., 1996; Bryar et al., 2000]. Together, the product $\rho(S/V)$ is called the surface relaxation rate, and reflects the effect of both pore geometry and geochemistry.

For practical reasons, T_1 measurements are difficult to make with borehole or surface NMR instruments, so field applications of NMR typically involve measurements of T_2. The transverse relaxation rate T_2^{-1} is the rate at which protons dephase as they return to equilibrium.

The expression for T_2^{-1} thus includes an additional term to account for internal magnetic field gradients (G) experienced by diffusing protons:

$$T_2^{-1} = T_{2B}^{-1} + \rho_2\left(S/V\right) + \frac{D}{12}\left(\gamma G t_E\right)^2 \tag{2}$$

Here ρ_2 is the transverse surface relaxivity, T_{2B}^{-1} is the relaxation rate of the bulk water, D is the self-diffusion coefficient of the water, γ is the gyromagnetic ratio of the hydrogen nucleus, and t_E is the echo-time, a timing parameter of the measurement. Relaxation in geologic materials with negligible magnetic susceptibility is dominated by surface relaxation in which case the expression for T_2^{-1} is reduced to simply

$$T_2^{-1} = \rho_2\left(S/V\right) \tag{3}$$

If we consider the NMR relaxation response of a single water-filled pore, the transverse magnetization signal is described by an exponential decay

$$M(t) = Ae^{-t/T_2} \tag{4}$$

where the initial signal amplitude A is proportional to the number of hydrogen nuclei (directly related to the pore volume). In a rock or sediment with a distribution of pore types, it is conventionally assumed that each pore contributes to the NMR signal in isolation and the net observed signal is modeled as multi-exponential decay

$$M(t) = \sum_i A_i \exp(-t/T_{2i}) \tag{5}$$

where the amplitude A_i is proportional to the volume of water-filled porosity associated with a corresponding relaxation time T_{2i}. Using this model of isolated pores, the $M(t)$ data are inverted to obtain a T_2 distribution, which is scaled according to Equation 3 to estimate a pore-size distribution assuming a uniform pore shape and surface relaxivity.

The simplest conceptualization of the isolated pore assumption is that each proton samples only one pore during the NMR measurement. D'Orazio et al. [1989] explained more completely that the isolated pore model is actually valid as long as the distance over which a proton will diffuse is smaller than the scale over which dissimilar pores (with different T_2) may be encountered. While this condition is generally satisfied for NMR measurements in consolidated sandstones with tight pore throats and relatively uniform pore bodies [Davis, 1990; Borgia et al., 1996], the model often breaks down for materials with well-connected heterogeneous pores. Hinedi et al. [1993, 1997] studied the NMR response of microporous near-surface materials, including soil aggregates and analogous synthetic silica gels, and noted that the size of larger intergranular pores was grossly underestimated. Although not recognized by the researchers, this error is most likely a consequence of pore coupling.

During a given time period T a proton will sample the pore network over an average diffusion length l, approximated as

$$l = \sqrt{6DT}\,, \tag{6}$$

where D is the self-diffusion coefficient of water (at 30ºC $D = 2.46 \times 10^{-9}$ m^2/s [Simpson and Carr, 1958]). Considering the duration of an NMR decay as represented by T_2 (typically 10-1000 ms), a proton may diffuse more than 100 μm during the NMR measurement. As the diffusion length approaches the scale at which dissimilar pores are encountered, pore coupling will begin to significantly complicate the NMR response. In the limiting case of infinite coupling, when the diffusion length is unbounded, the resulting T_2 distribution will exhibit a single peak representing $\rho S/V$ of the entire pore network [McCall et al. 1991]; however, the effect of pore coupling at intermediate strengths is poorly understood.

Ramakrishnan et al. [1999] modeled diffusional coupling in microporous grains and argued that the degree to which pores are coupled may be highly dependent on surface relaxivity. When ρ_2 is high, the diffusion length is reduced because enhanced relaxation limits the time and distance over which protons can travel before relaxing. Bryar et al. [2000] and Daughney et al. [2000] noted consistent results for laboratory measurements of T_1 in iron-coated silica gels. Surface coatings of paramagnetic Fe^{3+} increased ρ_1 of the gels by more than two orders of magnitude and significantly altered the shape of the relaxation time distributions. Our experiments here utilize a similar system of iron-coated silica gels to develop a range of samples between which the degree of pore coupling is expected to vary with iron concentration. NMR T_2 relaxation measurements on these samples should thus allow us to directly investigate the effects of pore coupling and explore the link between T_2 and pore geometry in heterogeneous materials.

METHODS AND MATERIALS

Sample characterization and preparation

The four samples used in this study are all derived from a high purity silica gel (Davisil® 150Å 60-200 mesh, Grace Davison) which has a bimodal pore-size distribution comprised of intragranular micropores (within the grains), reported to be ~15 nm in diameter, and larger intergranular macropores (between the grains). We first sieved the pure gel to achieve a narrower grain-size distribution of 53-105 μm. The diameter of intragranular pores in a random packing is estimated to be ~20 μm assuming a ratio of average pore size to grain size of 0.225 (Barker and Mehta, 1992). The micropore volume expressed as mL/g gel was provided from manufacturer specifications as 1.2 mL/g. We measured the surface area of the gels (315.1 ± 2.5

m^2/g) by the Brunauer-Emmett-Teller (BET) nitrogen adsorption method using a Micromeritics ASAP 2020 Accelerated Surface Area and Porosimetry System.

Our experimental approach was based on the assumption that increasing the amount of paramagnetic Fe^{3+} on the gel surface would reduce pore coupling by increasing the surface relaxation rate; therefore we closely controlled for surface geochemistry. We rinsed the gel repeatedly with 10% HCl and distilled, deionized (DDI) water (18 MΩ cm) to remove paramagnetic impurities and retained a portion of the cleaned gel to be used as the highest purity sample for NMR analysis. We then synthesized three additional gels with varied amounts of paramagnetic Fe^{3+} oxyhydroxide surface coating from the cleaned gel using methods of Grantham et al. [1997]. Samples were placed under vacuum and saturated with aqueous solutions of $FeSO_4$. The mixtures were then oxidized by the addition of excess 30% H_2O_2 and placed on an orbital shaker to equilibrate overnight. Following the iron coating treatment, the gels were rinsed with DDI water and oven dried overnight at 45°C. We determined the amount of paramagnetic Fe^{3+} sorbed to each gel from subsamples by atomic adsorption spectroscopy; concentrations of Fe^{3+} by mass in the four samples ranged from 0.00% in the pure sample to 0.10% in the most heavily coated sample. Qualitative analysis by scanning electron microscopy (SEM) and energy dispersion spectrometry (EDS) confirmed that iron was effectively sorbed to both the interior and exterior surfaces of the gels. Neither the porosity nor the surface area of the gels was changed, within experimental error, by the iron coating process.

NMR measurements

For NMR measurements, we packed dry samples of each gel in consistent weights and volumes into cylindrical Teflon sample holders with an interior diameter of 2.1 cm and height of 6 cm. In the first series of measurements, samples were completely saturated with DDI water.

To ensure maximum saturation, we first evacuated each packed sample in a dry vacuum (75 mmHg) for 30 minutes and then submerged the sample in a water bath before atmospheric pressure was restored. Samples were allowed to saturate for two hours while submerged. The volume of water held in micropores for each sample was calculated from the mass of dry sample (using manufacturer specified 1.2 mL/g gel); the volume of water in macropores was determined gravimetrically as the difference between total water volume and micropore volume. We determined that the total porosity was distributed with 58% of the total water volume held in micropores and 42% in the macropores.

We acquired a first series of NMR measurements directly after saturation. Following measurement at saturated conditions, we centrifuged the packed samples to drain water from the large intergranular pores. Centrifuging was found to remove approximately 98% of the intergranular pore water (estimated gravimetrically); the intragranular porosity was left undrained by this process due to the extremely high capillary potential of the micropores. We then acquired a second series of NMR measurements, immediately after centrifuging, at which point the NMR signal is presumed to be primarily sensitive to water in the undrained intragranular micropores.

All NMR relaxation data were collected using a 2.2MHz Maran Ultra NMR Core Analyzer (Resonance Instruments) with a CPMG pulse sequence. This instrument has a dead time of approximately 60 μs. Data were consistently acquired at 30°C and were stacked 100 times to improve the signal-to-noise ratio. Measurements at varied echo-time (t_E) spacing, indicated that magnetic gradient effects were negligible, therefore, the shortest available spacing t_E=150 μs was used to maximize data sampling at short times. Independent measurements on each sample were repeated three times to determine experimental variance.

We inverted each measured magnetization decay signal for a T_2 relaxation-time distribution using a regularized nonnegative least-squares algorithm developed after Whittall et al. [1991]. In this approach, the data are fit to 200 logarithmically spaced T_2 values, from 1 ms to 10 s, and the inverted model is regularized for smoothness. Regularization parameters were selected such that the data are fit to a tolerance equal to the measured noise level. This statistically robust approach is required to limit inversion artifacts and ensure that differences in the smoothness of the resulting T_2 distributions can be fairly ascribed physical significance.

RESULTS AND DISCUSSION

Laboratory NMR results

The four gels provide a group of samples with identical geometry and varied geochemistry, with ρ_2 expected to increase as iron content increases. An increase in ρ_2 was predicted to lead to a decrease in pore coupling as faster surface relaxation reduces the distance protons may diffuse before relaxing. Thus, analyzing these samples should allow us to assess the extent to which pore coupling may be controlled by surface geochemistry and how the coupling process affects the interpretation of NMR data.

The resulting T_2 distributions for each of the gel samples are shown in Figure 1 with iron concentrations increasing from top (0.000% Fe^{3+}) to bottom (0.010% Fe^{3+}). Solid curves show distributions for NMR measurements at fully saturated conditions; dashed curves are for measurements collected after centrifuging. Distributions for each sample are normalized by the total signal amplitude at full saturation which is consistent between all samples, to within experimental error.

Let us first consider the T_2 distributions for all four samples obtained after centrifuging, when the NMR measurement is exclusively sensitive to the saturated micropores. We note that the integrated amplitude of each distribution reflects 58% of the normalized signal; thus the total volume of microporosity is accurately captured. Despite the reported uniform intragranular pore size, we observe slightly broad peaks. Regularization of the inverted distributions may result in some peak broadening, however we have consistently found that inversions of data with high signal-to-noise (e.g. ~130 here) can produce narrow peaks when warranted by the data. We therefore interpret the breadth of the peaks as indicating that the size and surface-iron concentration of the micropores are not entirely uniform. For samples with increasing iron concentrations, we observe a shift of the centrifuged T_2 peak to shorter times, reflecting an expected increase in ρ_2. We calculate ρ_2 for each sample, listed in Table 1, from Equation 3 using the logarithmic mean relaxation time for each centrifuged distribution and independent measurements of S/V referenced previously.

Analyzing the T_2 distributions for measurements at full saturation next allows us to investigate the extent to which coupling occurs between the macropores and micropores. We begin with the results for the low-ρ_2 pure gel which we expect to exhibit the strongest degree of pore coupling. Given that the macropores and micropores differ in size by approximately three orders of magnitude, the isolated pore model would predict two distinct peaks in the relaxation-time distribution. Instead, we observe one broad peak with two marginally discernable modes separated by less than two orders of magnitude. This apparent averaging of the underlying pore-size distribution indicates that the two pore types are strongly coupled by diffusion. In the other three samples, as the concentration of iron coating the gel surface is increased, we observe a separation of the distribution into two clearly discernable modes or peaks, reflecting the

anticipated decrease in pore coupling. We note, however, that even for the most heavily iron-treated gel, the distance separating these peaks is still less than would be predicted by a purely isolated pore model.

Let us now explore the meaning of the relaxation-time distributions for these samples spanning a range of coupling strengths. We refer to the two modes in each distribution as the fast-relaxing signal (at lower T_2 values) and the slow-relaxing signal (at higher T_2 values). We find that for all samples, the fast-relaxing signal corresponds directly to the signal from the microporosity, represented in the centrifuged measurements. Thus, the relaxation time of the micropores is accurately reflected despite the presence of pore coupling and could be used to estimate a pore size assuming a given ρ_2-value. On the other hand, the location of the slow-relaxing signal, which should reflect the relative size of the macropores in the absence of pore coupling, overlaps the fast-relaxing micropore signal when pore coupling is strong and successively separates as the degree of pore coupling is reduced. Thus, when pore coupling is dominant, the relative size of the macropores would likely be dramatically underestimated.

In addition to this apparent shift in the position of the T_2-distributions, we observe that pore coupling also affects the relative amplitudes of the fast- and slow-relaxing signals. We estimate the relative volume of water relaxing at fast T_2, $\theta_{w\text{-}fast}$, versus slow T_2, $\theta_{w\text{-}slow}$, for each saturated sample by first splitting the distribution at the point of minimum slope and then integrating the distribution to the left and right, respectively. Values for the ratio $\theta_{w\text{-}fast}$:$\theta_{w\text{-}slow}$, estimated in this manner for each sample, are listed in Table 1. In the absence of pore coupling, we would expect $\theta_{w\text{-}fast}$:$\theta_{w\text{-}slow}$ to reflect the true ratio of micropore volume to macropore volume (1.37±0.04). For the pure gel, which exhibits the greatest degree of pore coupling, we find that the value $\theta_{w\text{-}fast}$:$\theta_{w\text{-}slow}$ under predicts the true ratio by 55%, grossly misrepresenting the true pore

geometry. As pore coupling weakens with increasing iron content, we see that the accuracy of this estimated ratio improves, eventually reaching 94% of the true value.

These laboratory observations are compatible with a conceptual model of pore coupling proposed by Ramakrishnan et al. [1999] in which protons move freely between intragranular micropores and intergranular macropores before relaxing. The leftward merging of the slow-relaxing peak for samples with low iron concentrations occurs because most protons which originate in macropores can freely diffuse into the microporous grains before relaxing. These protons thus relax at a much faster rate than would be predicted for isolated macropores and exhibit an averaging of rates for the two pore types. When surface relaxivity is high, fewer protons that originate in the macropores can efficiently sample the microporous region before relaxing, lessening the degree to which slow-relaxing peak is skewed leftward. The relative amplitude of the two peaks is likewise affected by the relative number of protons which sample both pore types. When relaxation occurs slowly, many protons are able to diffuse out of the smaller intragranular pores before relaxing, and so too decay at an averaged rate. For samples with substantial iron surface coatings, relaxation occurs rapidly and so a greater portion of protons originating in micropores relax before diffusing out of the grain; thus, the amplitude of the fast-relaxing T_2 peak more accurately represents the true micropore volume in these samples.

Comparison to analytical models

We can further compare our results quantitatively with the 1D model of pore coupling, presented by Ramakrishnan et al. [1999] and described fully therein. This model applies the NMR diffusion-reaction equation in two separate domains, one representing a microporous grain and one representing a macropore. The microporous grain, with radius R_g and porosity φ_μ, is treated as a continuum in which surface relaxation occurs at a specified rate $T_{2S\mu}$. To account for

restricted diffusion occurring within the micropores, the self-diffusion coefficient of water D is scaled by the formation factor of the microporous grain, F_μ. The total porosity of the system, φ_t, determines the dimensions of the two domains. The magnetization in the macropore domain, M_m, is governed by the standard NMR diffusion equation:

$$D\frac{d^2M_m}{dx^2} - M_m T_{2B}^{-1} = \frac{dM_m}{dt} \tag{7}$$

where again T_{2B} is the bulk water relaxation rate. The following equation describes M_μ, the magnetization in the domain of the microporous grain:

$$\frac{D}{F_\mu}\frac{d^2M_\mu}{dx^2} - \varphi_\mu M_\mu\left(T_{2S\mu}^{-1} + T_{2B}^{-1}\right) = \varphi_\mu \frac{dM_\mu}{dt} \tag{8}$$

A boundary condition between domains

$$D\frac{d^2M_m}{dx^2} = \frac{D}{F_\mu}\frac{d^2M_\mu}{dx^2} + \rho_2 M_m\left(1-\varphi_\mu\right) \tag{9}$$

matches flux into and out of the microporous grain and allows for relaxation at the grain wall with a surface relaxivity of ρ_2.

We fully parameterized four models to be representative of our measured samples. A value of T_{2B} = 3.05 s, consistently measured for all centrifuged fluids, was used across all models. Values for $(T_{2S\mu}^{-1}+T_{2B}^{-1})$ in Equation 8 are derived from the mean-log relaxation time for the micropores in each sample, measured after centrifuging. Representative values of ρ_2, obtained as described previously, are listed in Table 1. Geometric parameters R_g = 30 μm, φ_t = 0.83, and φ_μ= 0.725, reflect manufacturer specifications confirmed by independent measurements described previously. As it was not possible to directly measure F_μ, we selected a value of 1.4 ($1/\varphi_\mu$) consistent with an open, web-like network of pores typical of silica gels. We use a standard value of D = 2.46 x 10^{-9} m^2/s for water at 30ºC [Simpson and Carr, 1958].

Ramakrishnan [1999] explains that exact analytic solutions to the parameterized equations can be obtained using Laplace transforms and yield two principal exponential decay modes (smoothing effects are not modeled). However, obtaining analytic solutions is very challenging, so we instead use Comsol Multiphysics® to readily obtain accurate numerical solutions. In Figure 2, we plot the position and magnitude of the resulting principal decay modes superimposed over the experimental T_2 distributions for each sample. In general, we observe that modeled relaxation times closely predict the location of the T_2 peaks for laboratory measurements. We do, however, note that the relaxation time for the slow-relaxing peak is slightly overestimated in models representing the 0.004% and 0.010% Fe^{3+} gels. Plotted in Figure 3 and listed in Table 1 is a comparison of $\theta_{w\text{-}fast}$:$\theta_{w\text{-}slow}$, described previously, determined for each of the laboratory and modeled distributions (direct comparison is not possible in Figure 2 because the width of the experimental T_2 peaks is not constant). We plot modeled and experimental values along a 1:1 line in Figure 3 as filled circles with experimental error bars; the hollow diamond (top right) represents the true ratio value (1.37) which would be observed for zero pore coupling. We observe that modeled and experimental data are in considerable agreement; but we note that as iron concentrations increase, the modeled $\theta_{w\text{-}fast}$:$\theta_{w\text{-}slow}$ increasingly exceeds the experimental result. These minor disparities between modeled and laboratory results at higher iron concentrations suggest that the model may slightly overpredict the extent to which increased surface relaxivity can reduce pore coupling effects. Nonetheless, general agreement with our experimental results indicates that this relatively simple 1D model provides an accurate and extremely useful tool for predicting the NMR relaxation behavior in this class of heterogeneous media.

CONCLUSIONS

The NMR relaxation times of porous geological materials are closely linked to the volume and geometry of the water-saturated pore space. There is thus tremendous potential for using NMR relaxation measurements, acquired with borehole or surface-based instruments, in near-surface applications to estimate subsurface properties. It is clear, however, that substantial research is needed to fully understand the processes governing NMR relaxation in near-surface materials. This study has focused on the impact of pore coupling, a process which can significantly affect NMR relaxation measurements in systems with well-connected pores.

The experimental results presented in this paper conclusively demonstrate that surface geochemistry can be a significant factor determining the strength of pore coupling and thus the relationship between pore geometry and the NMR relaxation measurement. By controlling for surface geochemistry in well-characterized samples, we were able to directly assess the impact of pore coupling on the observed T_2 distribution in samples representing a range of coupling strengths. We find that for materials with intragranular microporosity and intergranular macroporosity, the effect of pore coupling is to reduce the slowest relaxation time associated with macropores and to decrease the amplitude of the fast-relaxing signal associated with the micropores. If unaccounted for in the interpretation of the NMR relaxation data, the presence of pore coupling would result in an underestimation of the total micropore volume and of the size of the largest pores. Good agreement between our laboratory results and an analytical model suggests that a theoretical approach may be useful for predicting the extent to which pore coupling will affect NMR measurements in other porous media.

This study has only considered the behavior of silica gels, which have smaller pores, and a lower ρ_2-value than is typical for most geological, unconsolidated materials. The small pores

will generally tend to limit the extent of the diffusion, while the low ρ_2-value will tend to enhance the extent of diffusion. While these properties of silica gel are different from those of a typical geological material, its well-characterized geometry has allowed us to investigate the link between surface chemistry and pore coupling. Our findings lead us to anticipate that for a wide class of unconsolidated materials with well-connected pores, the NMR relaxation-time distribution will not accurately convey the underlying pore structure due to pore coupling effects. Additional research is required to explore the impact of pore coupling in a broader range of materials in order to improve the interpretation of NMR data and advance the use of NMR methods in near-surface applications.

ACKNOWLEDGMENTS

We would like to thank the Stanford Surface and Aqueous Geochemistry Group for use of their surface area analyzer and Kristina Keating for assistance with the synthesis and analysis of iron coatings. This work was initiated with funding to Rosemary Knight under Grant DE-FG02-03ER15382-A0003 from the United States Department of Energy. Further funding was provided by Schlumberger Water Services. Elliot Grunewald was supported during this project by a scholarship from the ARCS foundation.

REFERENCES

Anand, Vivek and G.J. Hirasaki, 2007, Diffusional coupling between micro and macroporosity for NMR relaxation in sandstones and grainstones: Petrophysics, **48**, no. 4, 289-307.

Barker, G.C., and A. Mehta, 1992, Vibrated powders: Structures, correlations, and dynamics: Phys. Rev. A, **45**, 3435-3446.

Borgia, G.C., V. Bortolotti, A. F. Brancolini, R.J.S. Brown, and P. Fantazzini, 1996, Developments in core analysis by NMR measurements: Magnetic Resonance Imaging, **14**, no. 7/8, 751-760.

Brownstein, K.R., and C.E. Tarr, 1979, Importance of classical diffusion in NMR studies of water in biological cells: Physical Review A, **19**, no. 6, 2446-2453.

Bryar, T.R., C.J. Daughney, and R.J. Knight, 2000, Paramagnetic effects of iron(III) species on nuclear magnetic relaxation of fluid protons in porous media: Journal of Magnetic Resonance, **142**, 74-85.

Cohen, M.H., and K.S. Mendelson, 1981, Nuclear magnetic relaxation and the internal geometry of sedimentary rocks, Journal of Applied Physics, **53**, no. 2, 1127-1135.

Daughney, C.J., T.R. Bryar, R.J. Knight, 2000, Detecting sorbed hydrocarbons in a porous medium using proton nuclear magnetic resonance: Environ. Sci. Technol., **34**, no. 1, 332-337.

Davies, S., M.Z. Kalam, K.J. Packer, and F.O. Zelaya, 1990, Pore-size distributions from nuclear magnetic resonance spin-lattice relaxation measurements of fluid-saturated porous solids. II. Application to reservoir core samples: Journal of Applied Physics, **67**, no. 6, 3171-3176.

D'Orazio, F., J.C. Tarczon, W.P. Halperin, K. Eguchi, and T. Mizusaki, 1989, Application of nuclear magnetic resonance pore structure analysis to porous silica glass: Journal of Applied Physics, **65**, no. 2, 742-751.

Foley, I., S.A. Farooqui, and R.L. Kleinberg, 1996, Effect of paramagnetic ions on NMR relaxation of fluids at solid surfaces: J. Magn. Reson. A, **123**, 95-104.

Hertrich, M. 2008, Imaging of groundwater with nuclear magnetic resonance: Progress in

Nuclear Magnetic Resonance Spectroscopy, **541**, 227-248.

Hinedi, Z.R., Z.J. Kabala, T.H. Skaggs, D.B. Borchardt, R.W.K. Lee, and A.C. Chang, 1993, Probing soil and aquifer material porosity with nuclear magnetic resonance: Water Resources Research, **29**, no. 12, 3861-3866.

Hinedi, Z.R., A.C. Chang, M.A. Anderson, and D.B. Borchardt, 1997, Quantification of microporosiity by nuclear magnetic resonance relaxation of water imbibed in porous media: Water Resources Research, **33**, no. 12, 2697-2704.

Kenyon, W.E., P.I. Day, C. Straley, and J.F. Willemsen, 1988, A Three-Part Study of NMR Longitudinal Relaxation Properties of Water-Saturated Sandstones: SPE Formation Evaluation, **3**, no. 3.

Legchenko, A. and P. Valla, 2002, A review of the basic principles for proton magnetic resonance sounding measurements: Journal of Applied Geophyiscs, **50**, 3-19.

McCall, K.R., D.L. Johnson, and R.A. Guyer, 1991, Magnetization evolution in connected pore systems: Physical Review B, **44**, no. 14, 7344-7355.

Ramakrishnan, T.S., L.M. Schwartz, E.J. Fordham, W.E. Kenyon, and D.J. Wilkinson, 1999, Forward models for nuclear magnetic resonance in carbonate rocks: The Log Analysist, **40**, no. 4, 260-270.

Ramakrishnan, T.S., R. Ramamoorthy, E. Fordham, L. Schwartz, M. Herron, N. Saito, and A. Rabaute, 2001, A model-based interpretation methodology for evaluating carbonate reservoirs: SPE71704, New Orleans.

Seevers, D.O., 1966 A nuclear magnetic method for determining the permeability of sandstones: SPWLA Transactions, 7, Paper L.

Senturia, S.D., and J.D. Robinson, 1970, Nuclear spin-lattice relaxation of liquids confined in

porous solids, Society of Petroleum Engineering Journal: **10**, 237-244.

Simpson, J.H., and H.Y. Carr, 1958, Diffusion and nuclear spin relaxation in water: The Phyiscal Review, **111**, no. 5, 1201-1202.

Toumelin, E., C. Torres-Verdin, S. Chen, and D.M. Fischer, 2002, Analysis of NMR diffusion coupling effects in two-phase carbonate rocks: comparison of measurements with Monte Carlo simulations: SPWLA Transactions, 43rd Annual Logging Symposium, JJJ.

Walsh, D. O., 2008, Multi-channel surface NMR instrumentation and software for 1D/2D groundwater investigations: Journal of Applied Geophyiscs, **66**, 140-150.

Whittall, K.P., M.J. Bronskill, and R.M. Henkelman, 1991, Investigations of analysis techniques for complicated NMR relaxation data: Journal of Magnetic Resonance, **95**, 221-234.

Zielinksi, L.J., Y.-Q. Song, S. Ryu, and P.N. Sen, 2002, Characterization of coupled pore systems from the diffusion eigenspectrum: Journal of Chemical Physics, **117**, no. 11, 5361-5365.

FIGURE CAPTIONS

Figure 1 -- NMR relaxation-time distributions for the four silica gel samples labeled in the top left corner of each plot. Iron concentrations increase from top to bottom. Solid curves are for measurements at full saturation. Dashed curves are for measurements after centrifuging (signal exclusively from micropores). Curves for each sample are normalized by the initial signal amplitude for the fully saturated measurements.

Figure 2 -- Comparison between laboratory measurements and the simulated relaxation response based on the Ramakrishnan et al. [1999] 1D model. Solid curves are for laboratory measurements on gels at saturated conditions. Dashed bars show the position and amplitude of the primary exponential relaxation modes derived from the model. Mode amplitudes are all

normalized such that, for the pure gel, the long-time peak is exactly matched by the long-time mode.

Figure 3 -- Comparison of the value $\theta_{w\text{-}fast}$:$\theta_{w\text{-}slow}$ derived from laboratory and model-generated results. Estimates from laboratory measurements represent the ratio of integrated amplitude for the short-time peak to that of the long-time peak. Error bars show the standard deviation for this estimate from repeated measurements. Estimates from modeled data represent the ratio of the short-time mode amplitude to that of the long-time mode. The hollow black diamond (top-right) represents actual value of the micropore to macropore volume which would be reflected by $\theta_{w\text{-}fast}$:$\theta_{w\text{-}slow}$ in the absence of pore coupling effects.

Table 1 -- Tabulated estimates of geochemical properties for each sample and the estimated ratio $\theta_{w\text{-}fast}$:$\theta_{w\text{-}slow}$ for laboratory measurements and model data.

FIGURE 1

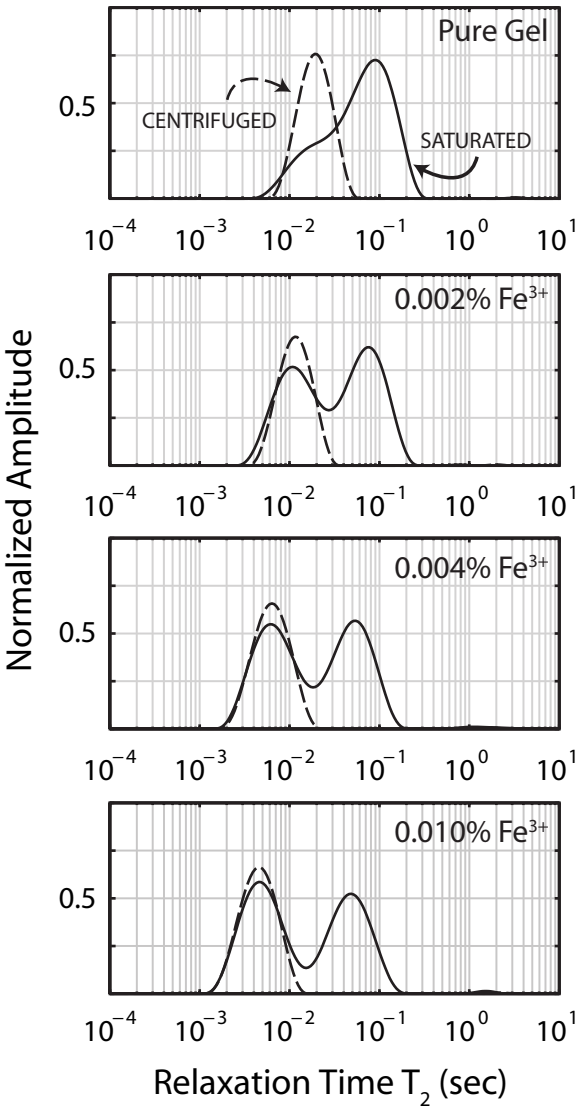
Pure Gel
CENTRIFUGED
SATURATED
0.002% Fe3+
0.004% Fe3+
0.010% Fe3+
0.5
10−4 10−3 10−2 10−1 100 101
Normalized Amplitude
Relaxation Time T2 (sec)

FIGURE 2

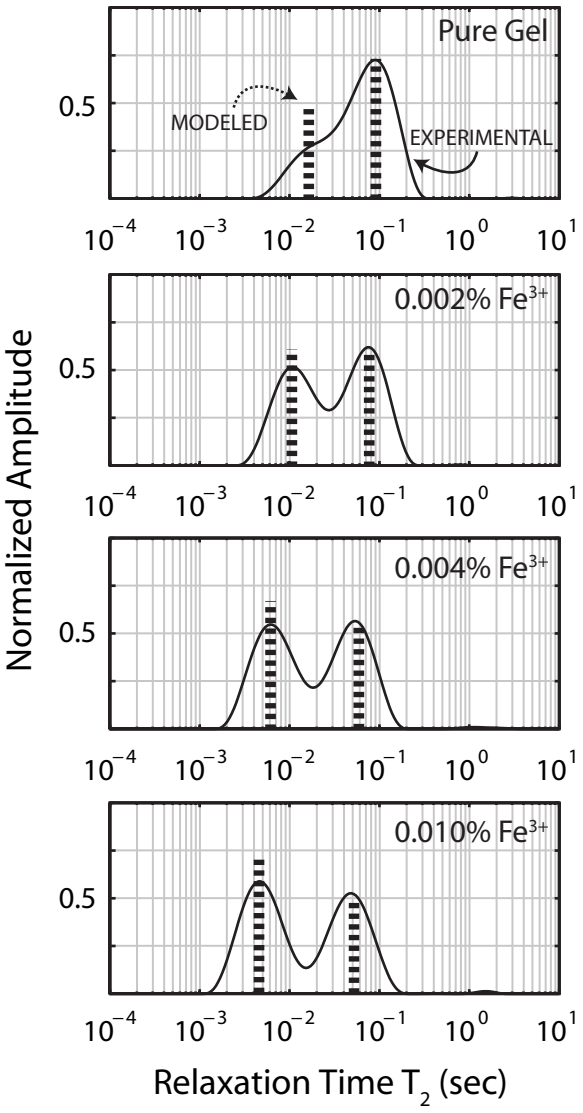
Pure Gel
MODELED
EXPERIMENTAL
0.002% Fe3+
0.004% Fe3+
0.010% Fe3+
0.5
10−4 10−3 10−2 10−1 100 101
Normalized Amplitude
Relaxation Time T2 (sec)

FIGURE 3

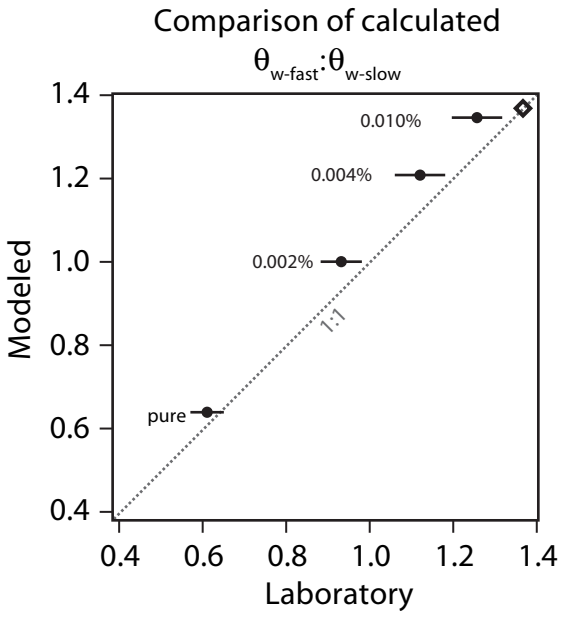
Comparison of calculated
θw-fast:θw-slow
Modeled
Laboratory
1.4
1.2
1.0
0.8
0.6
0.4
0.010%
0.004%
0.002%
pure
1:1

TABLE 1

% Fe^{3+} by mass	ρ_2 μm/s	$\theta_{w\text{-}fast}$:$\theta_{w\text{-}slow}$ laboratory	$\theta_{w\text{-}fast}$:$\theta_{w\text{-}slow}$ modeled
0.000%	0.201 ±0.007	0.61 ±0.04	0.64
0.002%	0.345 ±0.004	0.93 ±0.05	1.00
0.004%	0.592 ±0.010	1.12 ±0.06	1.21
0.010%	0.953 ±0.004	1.26 ±0.06	1.34